THE JOURNAL OF PHYSICAL CHEMISTRY C

Article

pubs.acs.org/JPCC

Investigation of Silica-Supported Vanadium Oxide Catalysts by High-Field ^{51}V Magic-Angle Spinning NMR

Nicholas R. Jaegers,[†,‡,⊥] Chuan Wan,[†,⊥] Mary Y. Hu,[†,⊥] Monica Vasiliu,[§] David A. Dixon,[§] Eric Walter,[†] Israel E. Wachs,[∥] Yong Wang,[*,†,‡] and Jian Zhi Hu[*,†]

[†]Institute for Integrated Catalysis and Earth and Biological Science Directorate, Pacific Northwest National Laboratory, Richland, Washington 99354, United States

[‡]Voiland School of Chemical Engineering and Bioengineering, Washington State University, Pullman, Washington 99163, United States

[§]Department of Chemistry, The University of Alabama, Tuscaloosa, Alabama 35487, United States

[∥]*Operando* Molecular Spectroscopy & Catalysis Laboratory, Department of Chemical & Biomolecular Engineering, Lehigh University, Bethlehem, Pennsylvania 18015, United States

Supporting Information

ABSTRACT: Supported V_2O_5/SiO_2 catalysts were studied using solid-state ^{51}V magic-angle spinning NMR at a sample spinning rate of 36 kHz and at a magnetic field of 19.975 T to provide a better understanding of the coordination of the vanadium oxide as a function of environmental conditions. Structural transformations of the supported vanadium oxide species between the catalyst in the dehydrated state and hydrated state under an ambient environment were revisited to examine the degree of oligomerization and the effect of water. The experimental results indicate the existence of a single dehydrated surface vanadium oxide species that resonates at −675 ppm and two vanadium oxide species under ambient conditions that resonate at −566 and −610 ppm. No detectable structural difference was found as a function of vanadium oxide loading on SiO_2 (3% V_2O_5/SiO_2 and 8% V_2O_5/SiO_2). Quantum chemistry simulations of the ^{51}V NMR chemical shifts on predicted surface structures were used as an aid in understanding potential surface vanadium oxide species on the silica support. The results suggest the formation of isolated surface VO_4 units for the dehydrated catalysts with the possibility of dimer and cyclic trimer presence. The absence of bridging V−O−V vibrations (~200−300 cm^{-1}) in previous Raman spectra, however, indicates that the isolated surface VO_4 sites are the dominant dehydrated surface vanadia species on silica. Upon exposure to water, hydrolysis of the bridging V−O−Si bonds is most likely responsible for the decreased electron shielding experienced by vanadium. No indicators for the presence of hydrated decavanadate clusters or hydrated vanadia gels previously proposed in the literature were detected in this study.

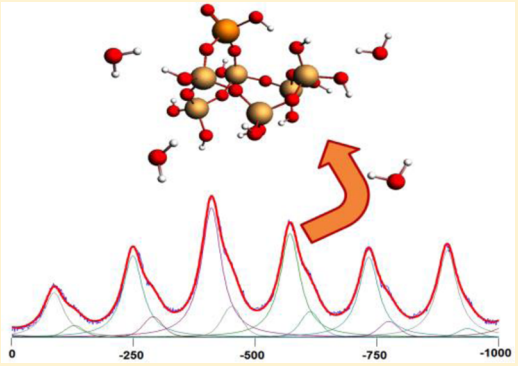

INTRODUCTION

Vanadium oxide catalysts have been identified as suitable materials in promoting a number of important chemical processes. Notable applications span a diverse collection of reactions including the selective oxidation of paraffins, olefins, and alcohols;[1] selective catalytic reduction of NO_x;[2] oxidation of a wide variety of organic molecules;[3] and oxidation of sulfur dioxide, a prevalent process for sulfuric acid manufacturing.[4] These catalysts have employed an assortment of oxide support materials such as zeolites, molecular sieves, bilayered and coprecipitated mixed oxides, and pure metal oxides, which are shown to impact the functionality of the catalyst and demonstrate improvements relative to the bulk V_2O_5 phase.[1] Ceria-supported vanadium, for instance, has shown turnover frequency (TOF) values higher by a factor of 10^3 than that of silica-supported vanadium oxide.[5] Although the TOF for silica is quite low, it is a supporting material that demonstrates high surface area relative to other oxide supports, making it a material of interest for catalytic applications. Additionally, it has been demonstrated that by augmenting the support with a layer of a second supporting material (bilayered catalysts), the reactivity can be enhanced by 2−3 orders of magnitude.[6] Understanding the nature of the surface of the catalytic material provides insights into the interaction between the catalyst and reactants, which are highly beneficial for understanding the specific roles of the chemical constituents; for comprehending how side products, such as water, might alter the chemistry of the reaction; and for rationally engineering better materials with enhanced performance. Uncertainties regarding the specific

Received: February 20, 2017
Revised: February 27, 2017
Published: February 27, 2017

DOI: 10.1021/acs.jpcc.7b01658
J. Phys. Chem. C 2017, 121, 6246−6254

nature of supported V_2O_5/SiO_2 catalysts still exist despite extensive investigation.[1]

Solid-state NMR is a spectroscopic technique that can probe the nuclei of solid structures to provide information about the coordination of the nuclear centers in addition to the chemical environment of the species present. As a spin I = 7/2 nucleus with a natural abundance of 99.75% and relatively short relaxation times, the ^{51}V nucleus is well-suited for spectroscopic NMR investigation. In this catalytic system, diamagnetic V^{5+} nuclei are present, making this an appropriate technique for analysis of the structure of supported vanadium oxide catalysts. Previously, solid-state NMR has been used to provide insight into supported VO_x/SiO_2 at a 79 MHz field and 8 kHz magic-angle spinning (MAS) rate.[7] Advances in technology have allowed for faster spinning rates, which narrow the lines of the spectrum by averaging the chemical shift anisotropy and eliminating first-order quadrupolar effects. Higher magnetic field strengths are also available to further improve spectral resolution through a reduction of second-order quadrupolar interactions. More advanced pulse sequences have also allowed for distinguished identification of overlapping sites.[8] Additional NMR studies have investigated the structure of silica-supported vanadium prepared by nontraditional methods, such as flame spray pyrolysis[9] and sodium promotion,[10] which demonstrate a higher monolayer capacity (3.3 and 8.9 V/nm^2) than traditional methods, and surface organometallic chemistry approaches that impact catalytic activity.[11] These studies all suggest the presence of isolated VO_4 units for dehydrated catalysts, and the flame spray work briefly speculates on the impact of hydration. In this study, we take advantage of high-field (19.975 T) MAS NMR at spinning rates above 30 kHz and couple the experiments with quantum chemical calculations to provide structural insights into the hydrated and dehydrated surface vanadium oxide phase of the supported V_2O_5/SiO_2 catalytic system prepared by traditional methods.

Prior investigations of the molecular structure of supported vanadium oxide catalysts noted significant structural changes between a dehydrated sample and one that was exposed to ambient conditions. This was demonstrated conclusively by in situ Raman spectroscopy of vanadium oxide supported on titania and alumina.[12] Early characterization of the dehydrated phase demonstrated the significance of Raman spectroscopy's sensitivity over X-ray diffraction (XRD) due to the relatively long-range crystallographic order required for detection with XRD.[13] In addition to Raman, in situ extended X-ray absorption fine structure (EXAFS) spectroscopy has been a key tool in understanding the structure of the surface vanadium oxide species in catalysts. EXAFS and Raman spectroscopies were used in conjunction with reference compounds to propose the presence of isolated $O{=}V(-O-Si)_3$ surface units up to monolayer coverage and the additional presence of crystalline V_2O_5 nanoparticles above this threshold.[14] In situ infrared spectroscopy was also utilized to demonstrate this, but with limited success due to signal overlap with the silica support and challenges with peak assignments.[15−17] Unlike other oxide supports, which have demonstrated oligomerization of surface vanadium oxide as loading increases, contrasting conclusions exist for the silica support's propensity to aid in the formation of surface vanadium oxide oligomers because of the dominance of isolated surface VO_x sites, as evidenced by Raman (absence of V−O−V vibrations at 200−300 cm^{-1}) and ultraviolet−visible (UV−vis) diffuse reflectance spectroscopy (DRS) (high E_g values) studies.[8,18] For alumina- and zirconia-supported vanadium oxide catalysts, as the loading of vanadium oxide increases, the structure of the surface vanadium oxide species becomes increasingly oligomeric until crystalline V_2O_5 nanoparticles are present. This was not observed for silica-supported vanadium oxide up to the saturation limit of 2.7 V/nm^2, lower than most oxide supports (~8 V/nm^2).[19] Another study suggests the superiority of UV−vis over Raman spectroscopy in this application due to strong coupling between the support and vanadia and concludes that differences in the degree of oligomerization with loading may be visible with UV−vis, but not detectable using Raman spectroscopy.[20] Furthermore, two recent EXAFS studies have supported the notion that higher surface vanadium oxide loading on silica leads to a greater degree of oligomerization up to the monolayer limit, but additional demonstration with model compounds is still required for greater support of this claim.[21,22] Multiwavelength Raman has identified a second monomeric surface VO_x species on silica at submonolayer coverage that has been predicted to be a partially hydroxylated vanadium oxide center.[23]

The hydrated phase of supported vanadium oxide catalysts is more complex. X-ray absorption near edge spectroscopy (XANES) and Raman spectroscopy have confirmed that the structure does indeed change upon hydration and that V_2O_5-like structures develop under this condition.[14,24] One hypothesis suggested to describe this change claims that the observed ^{51}V NMR chemical shift arises from a five-coordinated tetrahedral structure where water also coordinates.[9] Another relates the system to a phase diagram which demonstrates that the nature of surface vanadium oxide under hydrated conditions depends on the pH of the solution and concentration of vanadium oxide.[25] As the presence of vanadium oxide increases, causing the pH of the wet surface to decrease, oligomerization is facilitated through decavanadate clusters until bulklike vanadium oxide is formed. The presence of these decavanadate structures have been previously proposed based on Raman spectroscopy.[26] The concept of hydrolysis has also been investigated, and it has been proposed that the presence of sufficient ambient moisture may hydrolyze the bridging V−O−Si bonds and that polymeric vanadium oxide species may form through olation, passing through V−OH−V bridges until $V_2O_5{*}(H_2O)_n$ gels form.[14] Further Raman analysis demonstrated the partial reversibility of this hydration process and has asserted that this can occur without large amounts of water.[27] The present work further investigates structural insights about supported V_2O_5/SiO_2 catalysts with solid-state ^{51}V NMR given the recent advances achieved with this molecular spectroscopy.

METHODS

Sample Preparation. The silica support used for this study was Cabosil EH-5. This fluffy material was pretreated with water in order to condense its volume for easier handling. The wet SiO_2 was dried at 120 °C and subsequently calcined at 500 °C overnight. The supported V_2O_5/SiO_2 catalysts were prepared by the incipient-wetness impregnation of 2-propanol solutions of vanadium isopropoxide ($VO(O\text{-}Pri)_3$, Alfa-Aesar, 97% purity). The preparation was performed inside a glovebox with continuously flowing N_2. The SiO_2 support was initially dried at 120 °C to remove the physisorbed water before impregnation. After impregnation, the samples were kept inside the glovebox with flowing N_2 overnight. The samples were subsequently dried in flowing N_2 at 120 °C for 1 h and 300 °C

DOI: 10.1021/acs.jpcc.7b01658
J. Phys. Chem. C 2017, 121, 6246−6254

for 1 h. Then, the samples were calcined in flowing air at 300 °C for 1 h and 450 °C for 2 h.

Prepared catalysts were transferred into individual glass tubes and capped with quartz wool for dehydration. The sample tubes were then placed inside a tubular glass vacuum chamber attached to a turbo molecular pump (Agilent TPS Compact) with the application of vacuum controlled by a bellows valve. Vacuum was slowly applied to the sample chamber until a pressure on the order of 10^{-6} Torr was achieved. The temperature of the sample was adjusted with a tube furnace (Thermolyne 21100) and monitored with an Omega MDSSi8 series benchtop indicator. The catalysts were heated at 300 °C for 3 h. After this time elapsed, the samples were cooled under vacuum and the chamber, sealed closed with the bellows valve, was moved to a N_2 purged glovebox for loading into the 1.6 mm pencil-type rotors. The sample color changed from yellow-brown to dark gray-blue upon dehydration, suggesting a change in the coordination environment of vanadium and the possible presence of V^{4+} species.[28]

BET Surface Analysis. Surface analysis was conducted with an ASAP 2020 (Micromeritics). The samples were degassed for 4 h at 200 °C before measurement. N_2 adsorption and desorption isotherms were acquired at −195.8 °C to determine the Brunauer−Emmett−Teller (BET) surface area. Between 0.12 and 0.20 g were used for each measurement.

Solid-State ^{51}V NMR Spectroscopy. All of the solid-state ^{51}V NMR experiments were performed on a Varian-Inova 850 MHz NMR spectrometer equipped with a commercial 1.6 mm pencil-type MAS probe, operating at a magnetic field of 19.975 T. The corresponding Larmor frequency was 223.367 MHz. The single-pulse MAS NMR experiments were acquired with a $\pi/2$ pulse width of 1.85 μs and a spectral width of 5 MHz at a sample spinning rates of 36, 30, and 28 kHz. Rotor-synchronized Hahn echo NMR experiments were performed to collect the ^{51}V MAS NMR spectra. A half echo time equal to one rotor period was used. Depending on the samples, 150, 00−330 000 scans were used with a 0.2 s recycle delay. All of the chemical shifts were externally referenced to the center-band of bulk V_2O_5 (−610 ppm relative to $VOCl_3$). All NMR measurements were carried out at 25 °C. Spectral deconvolution was conducted using the DMFIT program,[29] and a spinning sideband simulation was incorporated into this analysis.

Electronic Structure Calculations. To accompany the spectroscopic observations, NMR chemical shift calculations were conducted to assist in the interpretation of experimental results. Electronic structure simulations utilized the Amsterdam Density Functional (ADF) package.[30−32] The geometry was optimized utilizing the generalized gradient approximation with the dispersion-corrected Becke−Lee−Yang−Parr functional (GGA-BLYP-D).[33−35] The all-electron, triple-ζ, two-polarization function (TZ2P) was implemented as the basis set with Slater type functionals.[36] NMR calculations were conducted with density functional theory using the gauge independent atomic orbital (GIAO) approach based on the findings of the Ziegler group.[37−40] Scalar relativistic effects were included at the two-component zero-order regular approximation (ZORA) level for the NMR calculations with the BLYP functional.[41,42]

^{51}V NMR chemical shifts require a standard reference for direct comparison between the spectra and calculations. $VOCl_3$ has previously been shown to be an acceptable representative molecule for NMR calculations,[43,44] and we have used it as the ^{51}V NMR reference. The resulting calculated electronic shielding for $VOCl_3$ was −1962.8 ppm at the BLYP-D level and −1921 ppm at the BLYP/ZORA level. The resulting calculated shielding for a vanadium atom shift is given as δ_{obs} (ppm) = $\sigma_{ref}(VOCl_3, calc) - \sigma_{calc}$.

RESULTS

Experimental Solid-State ^{51}V MAS NMR Spectroscopy. Solid-state ^{51}V MAS NMR spectroscopy was conducted on two silica-supported vanadium oxide catalysts containing 3% and 8% V_2O_5/SiO_2. Specific surface area (SSA) and inductively coupled plasma (ICP) analyses for these two samples can be found in Table 1 and suggest that only the surface vanadium oxide species should be present because the surface density is maintained below 2.7 V/nm^2, which is the dispersion limit. The identification of the central band in the NMR spectra for each catalyst in both the dehydrated and ambient conditions can also be found in the Supporting Information. This determination was conducted by acquiring two spectra of the same sample at different spinning rates and noting which resonances remained unaltered by sample rotation dynamics.

Table 1. Quantitative Characteristics of V_2O_5/SiO_2 Hydrated Catalysts

sample name	ICP loading	SSA (m^2/g)	loading (V/nm^2)	% V as V^{4+}
3% V_2O_5/SiO_2	2.9%	285	0.6	2.5
8% V_2O_5/SiO_2	7.4%	240	1.7	3.1

Furthermore, because of concerns over potential reduction of the surface vanadium oxide species by the evacuation treatment, electron paramagnetic resonance (EPR) spectra were collected, which revealed only the reduced vanadium V^{+4} species (details available in the Supporting Information). These measurements revealed that up to 3.1% of the vanadium was present as reduced V^{4+} under both ambient conditions and upon dehydration. Paramagnetic vanadium species were previously shown to impact the visibility of diamagnetic vanadium with NMR.[45] It was shown that up to 70% of the vanadium within 10 Å of a V^{3+} center could not be detected; however, the authors noted a dramatically reduced effect for V^{4+}. A later study suggested that the noted impact was amplified because of the presence of direct V^{3+}−O−V^{5+} bonds and that the effect on dispersed vanadium should be less dramatic.[46] Furthermore, the average distances between vanadium atoms in our 3% and 8% samples are 14.6 and 8.7 Å, respectively, meaning the 3% V_2O_5/SiO_2 sample should not be impacted and the 8% sample contains species near the outer boundary. Considering our average vanadium surface density and V^{4+} concentration (Table 1) as well as the reduced impact of V^{4+}, it is likely that more than 96% of the vanadium environments are being accounted for in the solid-state ^{51}V MAS NMR spectra and reduction has had little, if any, impact on the surface structure and our observations.

The solid-state ^{51}V MAS NMR results for each catalyst are presented in Figure 1. Chemical shifts are listed for the central band of each spectrum, with spinning side bands, denoted by "*". The employed spinning rates for these samples were sufficient to allow distinguishing the central band peak from the spinning side bands. In the hydrated state, all samples exhibited major peaks at −566−67 ppm with a shoulder upfield at −610−13 ppm. The small peak at −610−13 ppm is often

DOI: 10.1021/acs.jpcc.7b01658
J. Phys. Chem. C 2017, 121, 6246−6254

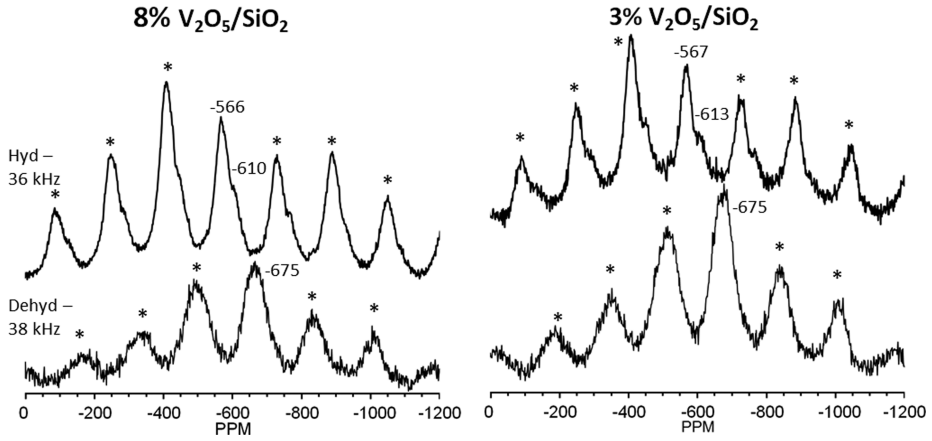

Figure 1. Solid-state ^{51}V MAS NMR of supported 8% and 3% VO_x/SiO_2 under hydrated (36 kHz) and dehydrated (38 kHz) conditions. Hydrated catalysts contain a major peak at −566−67 ppm and a shoulder at −610−13 ppm and were collected with 210k and 240k scans. Dehydrated catalysts exhibit a major peak at −675 ppm and were collected with 120k and 480k scans.

associated with a trace of crystalline V_2O_5 nanoparticles from minor agglomeration of the surface vanadium oxide species. Relatively little difference is observed between the samples in the hydrated state. Upon dehydration, a major peak at −675 ppm is present for the central band of each spectrum from the two catalysts. ^{1}H NMR spectra can be found in the Supporting Information and demonstrate a broad peak associated with water under ambient conditions. A very small peak indicating some quantity of residual water is present along with silanol protons that are seen in both samples.

The solid-state ^{51}V MAS NMR spectra presented in Figure 1 were fit with a Gaussian−Lorenzian model with a sideband simulation. The use of a quadrupolar model was not required to match the spectra because of the reduction in second-order quadrupolar interactions at the high magnetic field. The fitted models overlaid on each NMR spectrum can be viewed in the Supporting Information (Figures S4−S7). In each case, the central band, accompanying shoulders, and other peaks were fit with the Gaussian−Lorenzian model; the number of side bands and spinning rate were then specified. Each of the center and sideband constituents was integrated and normalized to the number of scans and the mass of the sample, and the calculated data are displayed in Table 2. As expected, the normalized area

Table 2. Integrated Area of Gaussian/Lorentzian Model Fits with a Side Band Simulation of ^{51}V NMR Spectra

condition	sample	mass (mg)	scans	normalized area
hydrated	3%	6.1	240k	231
hydrated	8%	7.4	210k	508
dehydrated	3%	4.9	480k	28
dehydrated	8%	4.7	120k	46

was smallest for the hydrated supported 3% V_2O_5/SiO_2 sample at a value of 231 (arbitrary unit). The hydrated supported 8% V_2O_5/SiO_2 sample indeed had a larger quantity of vanadium (508, arbitrary). Instead of the expected factor of 2.6, this sample contained ∼2.2 times as many V^{5+} nuclei as the 3% V_2O_5/SiO_2 catalyst. This suggests a possible slight over-representation in the 3% or an underrepresentation in the 8% sample. This same trend is true for the dehydrated case, suggesting it is not solely due to an oxidation state change during the dehydration process. The nearly order of magnitude difference in the normalized areas between the hydrated and dehydrated conditions results from the use of the echo experiment in the dehydrated samples as well as differences in the radio frequency tuning and impedance matching of the probe between these two sample groups. The ratios of the central band areas to total area (central band to sideband) are similar within each set.

The fractional comparison of all detected vanadium species for each sample are given in Table 3. The hydrated vanadium

Table 3. Integrated Peak Fractions for Each Modeled Species of the ^{51}V NMR Spectra

sample	−566	−610	−675
hyd 3%	0.842	0.158	–
hyd 8%	0.876	0.124	–
dehyd 3%	–	–	1.00
dehyd 8%	–	–	1.00

oxide catalysts consistently provide more than 84% as the −566 ppm species with the balance of the −610 ppm species. For the dehydrated vanadium oxide catalysts, both the supported 3% and 8% V_2O_5/SiO_2 samples have 100% of the detectable vanadium at −675 ppm.

Computational Modeling. We employed the BLYP exchange−correlation functional with dispersion which we previously used in a cluster model approach to analyze the chemical shifts of titania-supported vanadium oxide.[47] To further benchmark our approach, the chemical shifts of a set of model compounds were simulated and compared to experimental data (Table 4). As previously reported,[47] a model cluster of V_2O_5 containing eight vanadate atoms with a total charge of −5 was selected from the American Mineralogist Crystal Structure Database;[48] the terminal oxygen atoms were charge balanced and optimized to provide an estimate of the chemical shift of bulk V_2O_5. The solid-state ^{51}V NMR spectra of bulk vanadium oxide compare well with our quantum chemical calculation with a predicted shielding within 11 ppm of the experiment at BLYP-D level and within 13 ppm at the BLYP/ZORA level. The calculated chemical shifts on the vanadium-containing silsesquioxane agree with the reported experimental value[7] within 25 ppm at both levels. The predicted chemical shift for tris(triphenylsilyl) vanadate shows a larger discrepancy with the experiment[7] with deshielding differences up to 80 ppm. This may be due to enhanced

DOI: 10.1021/acs.jpcc.7b01658
J. Phys. Chem. C 2017, 121, 6246−6254

Table 4. Comparison of Experimental and Calculated Vanadium Chemical Shifts of Model Compounds[a]

compound	exptl.	BLYP-D	BLYP/ZORA
V_2O_5	−610	−633 (ave)	−636 (ave)
		−622 (center)	−624 (center)
$(Ph_3SiO)_3V{=}O$	−736[b]	−672	−656
$[(c\text{-}C_6H_{11})_7(Si_7O_{12})V{=}O]_2$	−714[b]	−700, −715	−690, −703

[a]All values are reported as parts per million relative to $VOCl_3$. [b]Results from Das et al.[7]

vanadyl (V═O) interactions with hydrogen molecules in the triphenylsilyl ligands in our model as compared to the powder samples. These benchmark calculations demonstrate that this approach can be reasonably utilized to provide insight on our experimental results.

The predicted chemical shift of a simple, neutral tetrahedral vanadium center ($VO(OH)_3$) of −574 ppm at the BLYP/ZORA level (Supporting Information) is predicted to be near the experimental result of −573 ppm. A tetrahedral positively charged $V(OH)_4^+$ structure is deshielded too much (−704 ppm, BLYP/ZORA) because of the excess positive charge. Negatively charged tetrahedral V sites are shielded too much with the ^{51}V chemical shift in $VO_2(OH)_2^{-1}$ being −498 ppm (BLYP/ZORA) and structures with more negative charges even more shielded. We thus explored larger structures with neutral tetrahedral vanadium sites. Geometries from our previous study of titanium-supported vanadium oxide with solid-state ^{51}V NMR spectra[47] were used as a starting point because they exhibited largely tetrahedral structures. Silicon was substituted for the titanium atoms, and geometries were optimized. The calculations (see Table S1) predicted chemical shifts that are significantly deshielded from those observed experimentally. The dehydrated isolated VO_4 unit is predicted to have a chemical shift of −459 ppm (BLYP-D) and −452 ppm (BLYP/ZORA), and the dimers are predicted to have chemical shifts between −580 and −590 ppm. Water-coordination to these model surfaces can increase or decrease shielding by about 20 ppm depending on the functional and inclusion of ZORA effects. As such, utilizing vicinal silanols as the anchoring sites for vanadium is not an appropriate model.

Larger clusters with at least O−Si−O bridges between silicon bonding sites were also considered. Table 5 shows the calculation results for dehydrated and hydrated monomer, dimer, and trimer species anchored to silicon atoms that possess a hydroxyl group. Figure 2 provides a visual representation of the cluster models used in these calculations

Table 5. Calculated ^{51}V NMR Chemical Shifts of Vanadium Clusters Relative to $VOCl_3$[a]

cluster	number of H_2O	BLYP-D dry	BLYP-D hydrated	BLYP/ZORA dry	BLYP/ZORA hydrated
monomer	2	−676	−669	−680	−673
dimer	4	−670	−631	−675	−635
		−672	−611	−678	−617
linear trimer	4	−515	−572	−537	−579
		−614	−656	−632	−661
		−619	−649	−636	−654
cyclic trimer	2	−661	−663	−661	−658
		−661	−682	−679	−675
		−706	−687	−703	−680

[a]Vanadium atoms are ordered to match dry with hydrated.

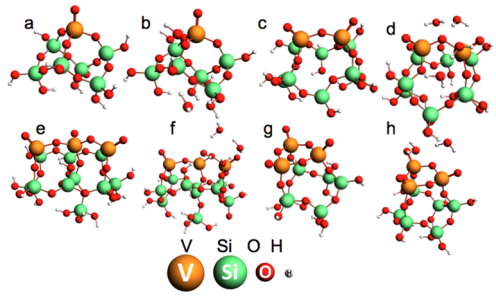

Figure 2. Optimized structures from Table 5: (a) monomer, (b) dihydrated monomer, (c) dimer, (d) tetra-hydrated dimer, (e) linear trimer, (f) tetra-hydrated linear trimer, (g) cyclic trimer, and (h) dihydrated cyclic trimer.

where the dehydrated and hydrated monomer (a, b), dimer (c, d), linear trimer (e, f), and cyclic trimer (g, h) are shown. Those with a full coordination sphere of siloxane can be found in the Supporting Information. Water molecules were added to the cluster to simulate a hydrated environment to predict the changes in chemical shifts upon water coordination (Table 5).

The monomer has a predicted chemical shift of −675 ppm in the hydroxyl case with both approaches. The siloxane $Si(OH)_3$ ligands fold upward, leading to interaction with the vanadium, deshielding the nucleus. Because the coordination environment around the surface silicon restricts the hydroxyl ligand interactions with vanadium, this provides a less distorted picture of the chemical environment. For this reason, the hydroxyl cases are analyzed exclusively within this text. Two water molecules were added to the system and coordinated with the VO_4 unit, which resulted in a shift downfield of about 7 ppm with both approaches. Chemical shift values centered on −671 ppm were calculated for the dimer. Once hydrated, the difference between the chemical shifts of the two vanadium atoms in the dimer increases to about 20 ppm (centered at −621 for BLYP-D and −626 ppm for the BLYP/ZORA). In the linear trimer model, the central vanadium atom exhibited a chemical shift deshielded by nearly 100 ppm (BLYP-D) or 80 ppm (BLYP/ZORA) relative to the outer two vanadium atoms. Hydration changed the predicted chemical shifts to −572 and −653 ppm (BLYP-D) and to −579 and −658 ppm (BLYP/ZORA). Thus, the vanadium shifts become more shielded with water coordination instead of the usual deshielding predicted for other model clusters. In the cyclic trimer model, a modest deshielding was observed for the chemical shifts in both computational approaches when two water molecules were coordinated. Apart from the hydrated dimer structure at −620 ppm, further inclusion of water did not provide chemical shifts near the observed −610 ppm peak. When six water molecules are added to the dimer instead of four, the chemical shift decreased to −630 ppm.

The effect of the V−O−support bridge hydrolysis on the chemical shift was also investigated to test the hypothesis of a hydrolysis mechanism leading to the formation of vanadia-gels.

DOI: 10.1021/acs.jpcc.7b01658
J. Phys. Chem. C 2017, 121, 6246−6254

Table 6. Calculated ^{51}V NMR Chemical Shifts for Hydrated Cluster Models of Altered Surface Morphologies Due to the Hydrolysis of Anchoring Sites

cluster	number H_2O	BLYP-D dry	BLYP-D hydrated	BLYP/ZORA dry	BLYP/ZORA hydrated
digrafted monomer	4	−625	$3H_2O$: −574	−631	$3H_2O$: −579
			$4H_2O$: −619		$4H_2O$: −625
monografted monomer	8	−603	−510	−610	−516
nongrafted monomer	4	−492	−525	−499	−532
nongrafted dimer	2	−533	−550	−541	−594
		−550	−601	−557	−606
digrafted dimer	2	−560	−584	−567	−591
		−566	−589	−572	−594
V−$(OH)_2$−V bridge digrafted	4	−463	−488	−469	−516
		−508	−507	−514	−498

A hydrolyzed $VO_2(H_2O)_4^+$ cluster shows remarkable similarity to the primary chemical shift observed in our hydrated spectra (−575 ppm, BLYP/ZORA). This suggests that hydrolyzed structures may be promising identities for the structure of the hydrated material. A series of hydrolyzed monomer and dimer clusters was investigated by analyzing the progressive hydrolysis of support bridges and formation of V−O−V bonds. The results of these cluster calculations can be seen in Table 6; additional configurations are located in the Table S3. A visual representation of these structures can be seen in Figure 3a−m.

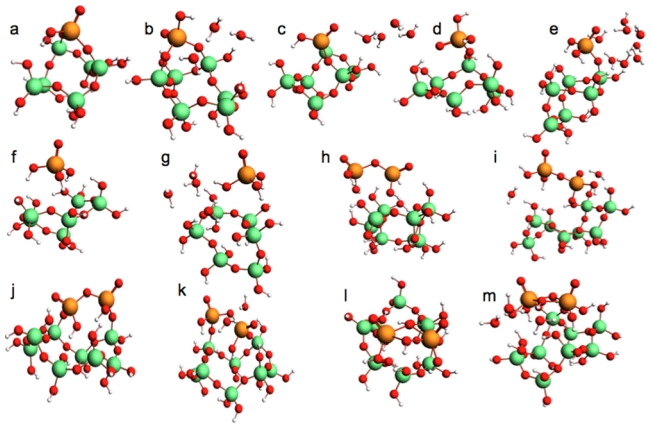

Figure 3. Optimized geometries from Table 6: (a) digrafted monomer, (b) trihydrated digrafted monomer, (c) tetra-hydrated digrafted monomer, (d) monografted monomer, (e) hydrated monografted monomer, (f) nongrafted monomer, (g) hydrated nongrafted monomer, (h) nongrafted dimer, (i) hydrated nongrafted dimer, (j) digrafted dimer, (k) hydrated digrafted dimer, (l) V−$(OH)_2$−V bridge digrafted dimer, and (m) hydrated V−$(OH)_2$−V bridge digrafted dimer.

Table 6 lists calculated chemical shifts for a variety of hydrolysis steps that were proposed by Gao et al.[14] and Xie et al.[27] In general, hydrolysis results in deshielded nuclear resonance relative to the anchored phase of the dehydrated state. Some interesting structures to note are the digrafted monomer structure with triple water coordination (Figure 3b) and the digrafted dimer (Figure 3j) (which has two bridge bonds hydrolyzed). Both of these show chemical shifts at the BLYP-D and BLYP/ZORA levels near the −566 ppm experimental value. Additionally, the dry digrafted monomer (Figure 3a) and the structure with four waters (Figure 3c) are predicted to have chemical shifts from about −620 to about −630 ppm at either computational level, similar to the chemical shift calculated for bulk vanadium oxide and the experimental chemical shift observed in the hydrated trials. Fully hydrolyzed isolated clusters (Figure 3e−i) resulted in chemical shifts near −500 ppm to −520 ppm, as did the V−$(OH)_2$−V cluster (Figure 3l,m). Structures with molecular water bridging between a monomer and dimer also were predicted for various separation distances between the two vanadium species. The results (Table S4) are consistent with the observation of deshielding relative to isolated monomer structures but do not appear to correspond to −566 ppm, with the most positive chemical shift for a monomer calculated at −590. The remaining cluster models demonstrate chemical shifts between −460 and −560 ppm.

DISCUSSION

The results of the solid-state ^{51}V MAS NMR spectra clearly show a change in the chemical environment for the vanadium nuclei for the supported V_2O_5/SiO_2 catalysts depending on the presence or absence of water. In general, the dehydrated supported V_2O_5/SiO_2 catalysts exhibit one major resonance at a chemical shift of −675 ppm as reported by Das et al.[7] and Grant et al.,[10] and similar to that of Love et al.[49] (−694 ppm). This somewhat contrasts the results of the flame-made and SOMC catalysts which show peaks at −715 and −615 ppm, respectively.[9,11] Each of these works ascribe the observed chemical shift to isolated VO_4 monomers. Upon hydration, a major peak at −566−67 ppm and a shoulder at −610−13 are detected. The NMR spectra clearly confirm the solid-state ^{51}V NMR spectra reported by Das et al.[7] and clarify the presence of a side peak in the hydrated sample as was reported by Schimmoeller et al.[9] The elemental analysis demonstrates the expected ratio of vanadium present in the 3% and 8% samples, although the 8% vanadium content appears to be slightly underrepresented in the ^{51}V NMR spectra relative to the 3% sample. No significant changes were noted between the NMR spectra of the 3% and 8% samples, suggesting that the structures of these two catalysts are similar given the difference in surface densities.

When these solid-state ^{51}V NMR spectra are compared to the calculated chemical shifts, the dehydrated state chemical shift closely resembles that of the monomer (VO_4) hydroxyl cluster, which was calculated at −676 ppm (BLYP-D) and at −680 ppm (BLYP/ZORA). The dehydrated dimer might also be present, with a calculated chemical shift of −671 (BLYP-D) and −676 ppm (BLYP/ZORA). The dehydrated linear trimer is not likely to be a potential morphology in these samples as the center vanadium atom is expected to have a significantly deshielded nucleus. This would translate to an additional downfield peak, corresponding to the central vanadium, of half

DOI: 10.1021/acs.jpcc.7b01658
J. Phys. Chem. C 2017, 121, 6246−6254

the intensity of the signal for the other two nuclei that is not seen in the spectra collected in this work. The dehydrated cyclic trimer may also be present as its average signal is −681 to −685 ppm. Raman spectra of dehydrated supported VO_x/SiO_2 catalysts, however, do not exhibit the presence of bridging V−O−V bonds, bending modes at ∼200−300 cm^{-1}, indicating that the isolated surface VO_4 sites on the SiO_2 support are the dominant surface vanadia species.[14] Tielens and colleagues noted the relative stability of trigrafted (isolated VO_4) units compared to mono- or digrafted species upon full dehydration, supporting our confirmation of isolated VO_4 units dominating the surface in the absence of water.[16]

The necessity of the nuclei anchoring to the silica support in larger rings that provide an O−Si−O bridge between anchoring sites should also be reiterated. This deduction is consistent with work by Tielens et al. in their investigation of model silica surfaces for supported vanadium oxide catalyst calculations. They conclude that three-ring silica sites tend to break open upon hydration in agreement with earlier conclusions from Raman spectroscopy showing selective consumption of the three-ring silica sites (∼605 cm^{-1}) upon anchoring of vanadia on silica.[8,50] This agrees with our prediction of larger rings as the anchoring sites for vanadium atoms.

The hydrated phase structure is less straightforward, as expected from conflicting previous literature reports. The solid-state ^{51}V NMR spectra reveal two peaks with chemical shifts near −566−67 and −610−13 ppm. The proposed hydrolysis of the V−O-support bonds leads to the observed species present in the hydrated NMR spectra. The variation in the number of linkages was investigated with theoretical calculations to gauge the stability of the various hydrolyzed structures. Tielens et al. found that under ambient hydration conditions, the mono- and digrafted species prevail, with the monografted species being the most stable up to 220 K and digrafted from 220 to 550 K. These thermodynamic calculations provide support for the preference for a digrafted over monografted in our system (at about 300 K) and could explain the experimental peak at −566 ppm. The results of our study do suggest the possibility of digrafted species being present with water coordination resonating at −567 and −625 ppm depending on how the water coordinates. The hydrated dimer species with two bridge bonds (digrafted dimer) also has a calculated chemical shift at −586 ppm (BLYP-D) and −592 ppm (BLYP/ZORA), which is similar to the observed value of −566 ppm. The hydrated nongrafted dimer may also be present. Given the difference in the calculated and observed model compounds, the hydrated dimer species with two bridge bonds cannot be eliminated as a possibly observed species. The small −610 ppm peak observed in these hydrated spectra is evidence of a bulk V_2O_5 component being present as crystalline nanoparticles because the samples were exposed to ambient conditions over a long period of time that tends to form some crystalline V_2O_5 nanoparticles. The loss of the minor −610 ppm band from the dehydrated catalysts indicates that the small V_2O_5 nanoparticles have likely dispersed upon the SiO_2 support during the dehydration−evacuation step.

Claims of the presence of hydrated decavanadate clusters and vanadia gels have also been considered in this study. Previous ^{51}V NMR reports of the chemical shift for the decavanadate structure have indicated that a minor peak at −426 ppm and major peaks at −512 and −531 ppm should be present for the diprotonated decavanadate structure.[51] Based on the phase diagram proposed by Baes and Messmer,[25] this should be the form present for a silica support, whose isoelectric point is typically between 2 and 3 on the pH scale. Additionally, our calculations on this structure for $[V_{10}O_{26}(OH)_2]^{4-}$, $[V_{10}O_{27}(OH)]^{5-}$, and $[V_{10}O_{28}]^{6-}$ (Table S5) show a distribution of peaks that is similar to those reported, but at less negative chemical shifts and dependent on the level of protonation. There is no support for this structure, however, because none of these peaks are found in the current solid-state ^{51}V NMR study.

Vanadia gels are more challenging to generalize. As an initial point, at least two distinct vanadia gel compounds have been identified based on the degree of hydration.[52,53] A second complication is the uncertainty surrounding the layered structure of these gels. While it has been hypothesized that the water takes up residence between the layers of the bulk species, other investigations have suggested two vanadium oxide layers with terminal oxygen atoms facing a water layer on either side of the bilayer.[54] Furthermore, reports concerning the ^{51}V chemical shift of these vanadia gel materials have varied greatly. The initial report by Nabavi et al. suggested that they resonated at −276 ppm.[55] In a later study, they recorded the static spectrum at −340 ppm.[56] With MAS, the spectra observed a broad isotropic shift resonating at −559 ppm.[57] Three more recent studies have found four peaks in the vanadia gel samples that resonate near −572, −593, −622, and −663 ppm.[58−60] Whereas the chemical shifts of these four peaks are near to peaks in our observed spectra, only two are actually observed in the current work. The previously observed −572 ppm peak is close to our observed −566 ppm peak, and the −622 ppm peak is reasonably close to our −610 ppm peak, but the other two peaks from vanadia gel (−593 and −663 ppm) were not observed in our spectra. The absence of the dual peak at the main feature or an upfield peak at −663 ppm suggests the assignment of the hydrated morphology is more likely to be the isolated, digrafted site or a digrafted dimer species, which would explain the increase in anisotropy relative to the isolated VO_4 unit assigned to the dehydrated sample. Our peak at −610 ppm likely correlates strongly with the bulk V_2O_5-like structures, which become dispersed again upon dehydration.

CONCLUSIONS

In this study, solid-state ^{51}V MAS NMR was utilized as a spectroscopic technique to probe the molecular structure of silica-supported vanadium oxide catalysts under dehydrated and hydrated conditions. Faster spinning rates at a higher field confirmed the previous results by Das et al.[7] and definitively demonstrated the presence of a side peak under ambient conditions. Dehydrated samples have a resonance at −675 ppm, while samples exposed to ambient conditions demonstrated two resonance peaks at −566 and −610 ppm. The results were the same for loadings of 3% and 8%, indicating no significant structural change with more than double the surface vanadium oxide coverage. Electronic structure calculations of the NMR chemical shifts for different models of potential vanadium oxide structures suggest the presence of isolated VO_4 units (and possibly dimers or cyclic trimers) for the dehydrated system; the presence of linear trimers is unlikely, consistent with earlier Raman studies demonstrating that the surface VO_x sites are isolated (absence of bridging V−O−V bonds). Upon hydration, we confirmed the deshielding effect of water coordination and have proposed that the observed species correspond to either digrafted monomers or dimers. The

DOI: 10.1021/acs.jpcc.7b01658
J. Phys. Chem. C 2017, 121, 6246−6254

oligomerization of the hydrated VO_x species is also reflected by the significant decrease in the UV−vis E_g value upon hydration,[14] which may be related to the presence V_2O_5-like structures. Digrafted monomers have previously been reported as stable under the conditions of our experiments. There is no indication of the presence of decavanadate clusters from the current experimental results coupled with chemical shift calculations, and there is only minimal support, if any, for the presence of vanadia gels.

■ ASSOCIATED CONTENT

Supporting Information

The Supporting Information is available free of charge on the ACS Publications website at DOI: 10.1021/acs.jpcc.7b01658.

Centerband determination experimental results; model fits of the NMR spectra under hydrated and dehydrated conditions; ^{1}H NMR spectra; calculated chemical shifts for additional molecular structures; optimized geometry coordinates; electron paramagnetic resonance spectra (PDF)

■ AUTHOR INFORMATION

Corresponding Authors

*E-mail: young.wang@pnnl.gov. Tel: 509-371-6273.
*E-mail: jianzhi.hu@pnnl.gov. Tel: 509-371-6544. Fax: 509-371-6546.

ORCID

David A. Dixon: 0000-0002-9492-0056
Jian Zhi Hu: 0000-0001-8879-747X

Author Contributions

⊥N.R.J., C.W., and M.Y.H. provided equal contributions.

Notes

The authors declare no competing financial interest.

■ ACKNOWLEDGMENTS

This research was supported by the U.S. Department of Energy, Office of Basic Energy Sciences, Division of Chemical Sciences, Biosciences, and Geosciences (DE-AC05-RL01830, FW-47319). Prof. I. E. Wachs (Lehigh University) was supported by the Center for Understanding & Control of Acid Gas-Induced Evolution of Materials for Energy (UNCAGE-ME), an Energy Frontier Research Center funded by DOE, Office of Science, Office of Basic Energy Sciences under Grant DE-SC0012577. NMR and EPR experiments were conducted in the Environmental Molecular Sciences Laboratory (EMSL), a national scientific user facility sponsored by the Department of Energy's Office of Biological and Environmental Research at Pacific Northwest National Laboratory (PNNL). The ^{1}H MAS NMR spectra were acquired using a Bruker 600 MHz NMR spectrometer acquired with support from the US Department of Energy, Office of Science, office of Basic Energy Sciences (Project Number 66628). EMSL's supercomputers were utilized as a resource for computational modeling. PNNL is a multiprogram national laboratory operated for the DOE by Battelle Memorial Institute under Contract DE-AC06-76RLO 1830. Elemental analysis was conducted at Galbraith Laboratories, Inc. The Seattle Chapter of the Achievement Rewards for College Scientists foundation is acknowledged for their fellow sponsorship of N. Jaegers. D. A. Dixon also thanks the Robert Ramsay Chair Fund of the University of Alabama for support.

■ REFERENCES

(1) Wachs, I. E. The Generality of Surface Vanadium Oxide Phases in Mixed Oxide Catalysts. *Appl. Catal., A* **2011**, *391*, 36−42.
(2) Wachs, I. E.; Deo, G.; Weckhuysen, B. M.; Andreini, A.; Vuurman, M. A.; Boer, M. d.; Amiridis, M. D. Selective Catalytic Reduction of NO with NH_3 over Supported Vanadia Catalysts. *J. Catal.* **1996**, *161*, 211−221.
(3) Wachs, I. E.; Jehng, J.-M.; Deo, G.; Weckhuysen, B. M.; Guliants, V. V.; Benziger, J. B.; Sundaresan, S. Fundamental Studies of Butane Oxidation over Model-Supported Vanadium Oxide Catalysts: Molecular Structure-Reactivity Relationships. *J. Catal.* **1997**, *170*, 75−88.
(4) Wachs, I. E. Catalysis Science of Supported Vanadium Oxide Catalysts. *Dalton Trans.* **2013**, *42*, 11762−11769.
(5) Wachs, I. E. Recent Conceptual Advances in the Catalysis Science of Mixed Metal Oxide Catalytic Materials. *Catal. Today* **2005**, *100*, 79−94.
(6) Lee, E. L.; Wachs, I. E. Surface Chemistry and Reactivity of Well-Defined Multilayered Supported $M_1O_x/M_2O_x/SiO_2$ Catalysts. *J. Catal.* **2008**, *258*, 103−110.
(7) Das, N.; Eckert, H.; Hu, H.; Wachs, I. E.; Walzer, J. F.; Feher, F. J. Bonding States of Surface Vanadium(V) Oxide Phases on Silica: Structural Characterization by Vanadium-51 NMR and Raman Spectroscopy. *J. Phys. Chem.* **1993**, *97*, 8240−8243.
(8) Lapina, O. B.; Shubin, A. A.; Khabibulin, D. F.; Terskikh, V. V.; Bodart, P. R.; Amoureux, J. P. Solid-State ^{51}V NMR for Characterization of Vanadium-Containing Systems. *Catal. Today* **2003**, *78*, 91−104.
(9) Schimmoeller, B.; Jiang, Y.; Pratsinis, S. E.; Baiker, A. Structure of Flame-Made Vanadia/Silica and Catalytic Behavior in the Oxidative Dehydrogenation of Propane. *J. Catal.* **2010**, *274*, 64−75.
(10) Grant, J. T.; Carrero, C. A.; Love, A. M.; Verel, R.; Hermans, I. Enhanced Two-Dimensional Dispersion of Group V Metal Oxides on Silica. *ACS Catal.* **2015**, *5*, 5787−5793.
(11) Barman, S.; Maity, N.; Bhatte, K.; Ould-Chikh, S.; Dachwald, O.; Haebner, C.; Saih, Y.; Abou-Hamad, E.; Llorens, I.; Hazemann, J. L.; et al. Single-Site VO_x Moieties Generated on Silica by Surface Organometallic Chemistry: A Way to Enhance the Catalytic Activity in the Oxidative Dehydrogenation of Propane. *ACS Catal.* **2016**, *6*, 5908−5921.
(12) Chan, S. S.; Wachs, I. E.; Murrell, L. L.; Wang, L.; Hall, W. K. In Situ Laser Raman Spectroscopy of Supported Metal Oxides. *J. Phys. Chem.* **1984**, *88*, 5831−5835.
(13) Roozeboom, F.; Mittelmeijer-Hazeleger, M. C.; Moulijn, J. A.; Medema, J.; De Beer, V. H. J.; Gellings, P. J. Vanadium Oxide Monolayer Catalysts. 3. A Raman Spectroscopic and Temperature-Programmed Reduction Study of Monolayer and Crystal-Type Vanadia on Various Supports. *J. Phys. Chem.* **1980**, *84*, 2783−2791.
(14) Gao, X.; Bare, S. R.; Weckhuysen, B. M.; Wachs, I. E. In Situ Spectroscopic Investigation of Molecular Structures of Highly Dispersed Vanadium Oxide on Silica under Various Conditions. *J. Phys. Chem. B* **1998**, *102*, 10842−10852.
(15) Magg, N.; et al. Vibrational Spectra of Alumina- and Silica-Supported Vanadia Revisited: An Experimental and Theoretical Model Catalyst Study. *J. Catal.* **2004**, *226*, 88−100.
(16) Islam, M. M.; Costa, D.; Calatayud, M.; Tielens, F. Characterization of Supported Vanadium Oxide Species on Silica: A Periodic DFT Investigation. *J. Phys. Chem. C* **2009**, *113*, 10740−10746.
(17) Keller, D. E.; Visser, T.; Soulimani, F.; Koningsberger, D. C.; Weckhuysen, B. M. Hydration Effects on the Molecular Structure of Silica-Supported Vanadium Oxide Catalysts: A Combined IR, Raman, UV−Vis and Exafs Study. *Vib. Spectrosc.* **2007**, *43*, 140−151.
(18) Tian, H.; Ross, E. I.; Wachs, I. E. Quantitative Determination of the Speciation of Surface Vanadium Oxides and Their Catalytic Activity. *J. Phys. Chem. B* **2006**, *110*, 9593−9600.
(19) Gao, X.; Bare, S. R.; Fierro, J. L. G.; Banares, M. A.; Wachs, I. E. Preparation and in-Situ Spectroscopic Characterization of Molecularly

DOI: 10.1021/acs.jpcc.7b01658
J. Phys. Chem. C 2017, 121, 6246−6254

Dispersed Titanium Oxide on Silica. *J. Phys. Chem. B* **1998**, *102*, 5653−5666.
(20) Bulánek, R.; Čičmanec, P.; Setnička, M. Possibility of VO_x/SiO_2 Complexes Speciation: Comparative Multi-Wavelength Raman and DR UV-Vis Study. *Phys. Procedia* **2013**, *44*, 195−205.
(21) Cavalleri, M.; Hermann, K.; Knop-Gericke, A.; Hävecker, M.; Herbert, R.; Hess, C.; Oestereich, A.; Döbler, J.; Schlögl, R. Analysis of Silica-Supported Vanadia by X-Ray Absorption Spectroscopy: Combined Theoretical and Experimental Studies. *J. Catal.* **2009**, *262*, 215−223.
(22) Zhu, H.; Ould-Chikh, S.; Dong, H.; Llorens, I.; Saih, Y.; Anjum, D. H.; Hazemann, J.-L.; Basset, J.-M. VO_x/SiO_2 Catalyst Prepared by Grafting $VOCl_3$ on Silica for Oxidative Dehydrogenation of Propane. *ChemCatChem* **2015**, *7*, 3332−3339.
(23) Wu, Z.; Dai, S.; Overbury, S. H. Multiwavelength Raman Spectroscopic Study of Silica-Supported Vanadium Oxide Catalysts. *J. Phys. Chem. C* **2010**, *114*, 412−422.
(24) Yoshida, S.; Tanaka, T.; Hanada, T.; Hiraiwa, T.; Kanai, H.; Funabiki, T. Analysis of XANES for Identification of Highly Dispersed Transition Metal Oxides on Supports. *Catal. Lett.* **1992**, *12*, 277−285.
(25) Baes, C. F.; Messmer, R. E. *The Hydrolysis of Cations*; John Wiley & Sons Inc.: New York, 1976.
(26) Deo, G.; Wachs, I. E. Predicting Molecular Structures of Surface Metal Oxide Species on Oxide Supports under Ambient Conditions. *J. Phys. Chem.* **1991**, *95*, 5889−5895.
(27) Xie, S.; Iglesia, E.; Bell, A. T. Effects of Hydration and Dehydration on the Structure of Silica-Supported Vanadia Species. *Langmuir* **2000**, *16*, 7162−7167.
(28) Haber, J. Fifty Years of My Romance with Vanadium Oxide Catalysts. *Catal. Today* **2009**, *142*, 100−113.
(29) Massiot, D.; Fayon, F.; Capron, M.; King, I.; Le Calvé, S.; Alonso, B.; Durand, J.-O.; Bujoli, B.; Gan, Z.; Hoatson, G. Modelling One- and Two-Dimensional Solid-State NMR Spectra. *Magn. Reson. Chem.* **2002**, *40*, 70−76.
(30) te Velde, G.; Bickelhaupt, F. M.; Baerends, E. J.; Fonseca Guerra, C.; van Gisbergen, S. J. A.; Snijders, J. G.; Ziegler, T. Chemistry with ADF. *J. Comput. Chem.* **2001**, *22*, 931−967.
(31) Fonseca Guerra, C.; Snijders, G. J.; te Velde, G.; Baerends, J. E. Towards an Order-N DFT Method. *Theor. Chem. Acc.* **1998**, *99*, 391−403.
(32) *ADF2014 SCM*; Vrije Universiteit: Amsterdam, The Netherlands, 2014; http://www.scm.com.
(33) Lee, C.; Yang, W.; Parr, R. G. Development of the Colle-Salvetti Correlation-Energy Formula into a Functional of the Electron Density. *Phys. Rev. B: Condens. Matter Mater. Phys.* **1988**, *37*, 785−789.
(34) Becke, A. D. Density-Functional Exchange-Energy Approximation with Correct Asymptotic Behavior. *Phys. Rev. A: At., Mol., Opt. Phys.* **1988**, *38*, 3098−3100.
(35) Grimme, S.; Antony, J.; Schwabe, T.; Muck-Lichtenfeld, C. Density Functional Theory with Dispersion Corrections for Supramolecular Structures, Aggregates, and Complexes of (Bio)Organic Molecules. *Org. Biomol. Chem.* **2007**, *5*, 741−758.
(36) Van Lenthe, E.; Baerends, E. J. Optimized Slater-Type Basis Sets for the Elements 1−118. *J. Comput. Chem.* **2003**, *24*, 1142−1156.
(37) Wolinski, K.; Hinton, J. F.; Pulay, P. Efficient Implementation of the Gauge-Independent Atomic Orbital Method for NMR Chemical Shift Calculations. *J. Am. Chem. Soc.* **1990**, *112*, 8251−8260.
(38) Schreckenbach, G.; Ziegler, T. Calculation of NMR Shielding Tensors Using Gauge-Including Atomic Orbitals and Modern Density Functional Theory. *J. Phys. Chem.* **1995**, *99*, 606−611.
(39) Schreckenbach, G.; Ziegler, T. Calculation of NMR Shielding Tensors Based on Density Functional Theory and a Scalar Relativistic Pauli-Type Hamiltonian. The Application to Transition Metal Complexes. *Int. J. Quantum Chem.* **1997**, *61*, 899−918.
(40) Wolff, S. K.; Ziegler, T.; van Lenthe, E.; Baerends, E. J. Density Functional Calculations of Nuclear Magnetic Shieldings Using the Zeroth-Order Regular Approximation (ZORA) for Relativistic Effects: Zora Nuclear Magnetic Resonance. *J. Chem. Phys.* **1999**, *110*, 7689−7698.
(41) Lenthe, E. v.; Baerends, E. J.; Snijders, J. G. Relativistic Regular Two-Component Hamiltonians. *J. Chem. Phys.* **1993**, *99*, 4597−4610.
(42) Autschbach, J.; Ziegler, T. In *Calculation of NMR and EPR Parameters: Theory and Applications*; Wiley-VCH & Co.: Weinheim, 2004; pp 249−264.
(43) Bjornsson, R.; Fruchtl, H.; Buhl, M. ^{51}V NMR Parameters of $VOCl_3$: Static and Dynamic Density Functional Study from the Gas Phase to the Bulk. *Phys. Chem. Chem. Phys.* **2011**, *13*, 619−627.
(44) Justino, L. L. G.; Ramos, M. L.; Kaupp, M.; Burrows, H. D.; Fiolhais, C.; Gil, V. M. S. Density Functional Theory Study of the Oxoperoxo Vanadium(V) Complexes of Glycolic Acid. Structural Correlations with NMR Chemical Shifts. *Dalton Trans.* **2009**, 9735−9745.
(45) Shubin, A. A.; Lapina, O. B.; Bosch, E.; Spengler, J.; Knözinger, H. Effect of Milling of V_2O_5 on the Local Environment of Vanadium as Studied by Solid-State ^{51}V NMR and Complementary Methods. *J. Phys. Chem. B* **1999**, *103*, 3138−3144.
(46) Lapina, O. B.; Shubin, A. A.; Nosov, A. V.; Bosch, E.; Spengler, J.; Knözinger, H. Characterization of V_2O_5−TiO_2 Catalysts Prepared by Milling by ESR and Solid State ^{1}H and ^{51}V NMR. *J. Phys. Chem. B* **1999**, *103*, 7599−7606.
(47) Hu, J. Z.; et al. Investigation of the Structure and Active Sites of TiO_2 Nanorod Supported VO_x Catalysts by High-Field and Fast-Spinning ^{51}V Mas NMR. *ACS Catal.* **2015**, *5*, 3945−3952.
(48) Downs, R. T.; Hall-Wallace, M. The American Mineralogist Crystal Structure Database. *Am. Mineral.* **2003**, *88*, 247−250.
(49) Love, A. M.; Carrero, C. A.; Chieregato, A.; Grant, J. T.; Conrad, S.; Verel, R.; Hermans, I. Elucidation of Anchoring and Restructuring Steps During Synthesis of Silica-Supported Vanadium Oxide Catalysts. *Chem. Mater.* **2016**, *28*, 5495−5504.
(50) Tielens, F.; Gervais, C.; Lambert, J. F.; Mauri, F.; Costa, D. Ab Initio Study of the Hydroxylated Surface of Amorphous Silica: A Representative Model. *Chem. Mater.* **2008**, *20*, 3336−3344.
(51) Pozarnsky, G. A.; McCormick, A. V. ^{51}V NMR and EPR Study of Reaction Kinetics and Mechanisms in V_2O_5 Gelation by Ion Exchange of Sodium Metavanadate Solutions. *Chem. Mater.* **1994**, *6*, 380−385.
(52) Repelin, Y.; Husson, E.; Abello, L.; Lucazeau, G. Structural Study of Gels of V_2O_5: Normal Coordinate Analysis. *Spectrochim. Acta Part, A: Molecular Spectroscopy* **1985**, *41*, 993−1003.
(53) Abello, L.; Husson, E.; Repelin, Y.; Lucazeau, G. Structural Study of Gels of V_2O_5: Vibrational Spectra of Xerogels. *J. Solid State Chem.* **1985**, *56*, 379−389.
(54) Kristoffersen, H. H.; Metiu, H. Structure of $V_2O_5{\cdot}nH_2O$ Xerogels. *J. Phys. Chem. C* **2016**, *120*, 3986−3992.
(55) Nabavi, M.; Taulelle, F.; Sanchez, C.; Verdaguer, M. XANES and ^{51}V NMR Study of Vanadium-Oxygen Compounds. *J. Phys. Chem. Solids* **1990**, *51*, 1375−1382.
(56) Nabavi, M.; Sanchez, C.; Livage, J. Structure and Properties of Amorphous V_2O_5. *Philos. Mag. B* **1991**, *63*, 941−953.
(57) Luca, V.; Hook, J. M. Study of the Structure and Mechanism of Formation through Self-Assembly of Mesostructured Vanadium Oxide. *Chem. Mater.* **1997**, *9*, 2731−2744.
(58) Fontenot, C. J.; Wiench, J. W.; Pruski, M.; Schrader, G. L. Vanadia Gel Synthesis Via Peroxovanadate Precursors. 2. Characterization of the Gels. *J. Phys. Chem. B* **2001**, *105*, 10496−10504.
(59) Fontenot, C. J.; Wiench, J. W.; Schrader, G. L.; Pruski, M. ^{17}O Mas and 3QMAS NMR Investigation of Crystalline V_2O_5 and Layered $V_2O_5{\cdot}nH_2o$ Gels. *J. Am. Chem. Soc.* **2002**, *124*, 8435−8444.
(60) Durupthy, O.; Steunou, N.; Coradin, T.; Maquet, J.; Bonhomme, C.; Livage, J. Influence of pH and Ionic Strength on Vanadium(V) Oxides Formation. From $V_2O_5{\cdot}nH_2O$ Gels to Crystalline $NaV_3O_8{\cdot}1.5H_2O$. *J. Mater. Chem.* **2005**, *15*, 1090−1098.

DOI: 10.1021/acs.jpcc.7b01658
J. Phys. Chem. C 2017, 121, 6246−6254